Electronic Supplementary Information (ESI)

Facile one-pot synthesis of colloid stable, monodispersed, highly PEGylated $CuS@mSiO_2$ nanocomposites for the combination of photothermal and chemotherapy

Feng Lu, Jinfeng Wang, Lin Yang, and Jun-Jie Zhu*

State Key Lab. of Analytical Chemistry for Life Science, School of Chemistry and Chemical Engineering, Nanjing University, Nanjing 210093, P. R. China. E-mail: jjzhu@nju.edu.cn; Fax: (+86)-25-8359-7204; Tel: (+86)-25-8359-7204

Experimental section

Chemicals: Copper chloride ($CuCl_2$), Hexadecyltrimethylammonium bromide (CTAB), sodium sulfide (Na_2S), tetraethyl orthosilicate (TEOS), ethyl acetate, sodium chloride (NaCl), Hydrogen tetrachloroaurate trihydrate ($HAuCl_4$), sodium oleate, silver nitrate ($AgNO_3$), ascorbic acid, sodium borohydride ($NaBH_4$), ethanol and chloroform were purchased from Sinopharm Chemical Reagent Co., Ltd. Ammonium nitrate were obtained from Xiya Reagent. Doxorubicin hydrochloride (DOX) was purchased from Sangon Biotech. 2-[Methoxy(polyethyleneoxy)$_{9\text{-}12}$propyl] trimethoxysilane (PEG-silane) were obtained from J&K Scientific Ltd. Calcein AM, Propidium Iodide (PI) and 3-(4,5-dimethylthiozol-2-yl)-2,5-diphenyltetrazolium bromide (MTT) were purchased from KeyGEN BioTECH. All the chemicals were used as received without further purification.

Characterization: Transmission electron microscopy (TEM) images were obtained with a JEOL JEM 1011 electron microscope at an acceleration voltage of 100 kV. X-ray powder diffraction (XRD) measurements were performed on a Shimadzu XRD-6000 with Cu Kα radiation (λ = 0.15418 nm) with a scanning rate of 2 deg/min. UV-Vis spectra were recorded using a UV-3600 spectrophotometer (Shimadzu). The fluorescence intensity was measured on RF-5301PC fluorescence spectrometer. FTIR spectra were taken on a Nicolet 6700 spectrograph. Dynamic light scattering (DLS) was performed on BI-200SM Laser Light Scattering Instrument (Brookhaven). Confocal laser scanning microscopy (CLSM) images were obtained using a Leica TCS SP5 microscope.

Synthesis of $CuS@mSiO_2$-PEG nanoparticles: Na_2S (50 mM, 1mL) and $CuCl_2$ (50 mM, 1mL) aqueous solution were injected into a 48 mL CTAB aqueous solution (0.125 mg/mL) in a 100 mL three neck flask, forming a brown homogenous solution. After stirring for 15 min, the solution was degassed and heated to 90 ^oC under a genteel nitrogen flow. The solution turned into dark green gradually and the temperature was maintained at 90 ^oC for 1 hour to obtain CTAB stabilized CuS nanoparticles. Subsequent, the solution was cooled to 70 ^oC and another portion of CTAB was added to make the total CTAB concentration at 2 mg/mL. After 15 min stir, 350 uL of NaOH (2M), 200 uL of TEOS and 1 mL of ethyl acetate were injected into the solution quickly to coat a

mesoporous silica layer on CuS. 70 uL PEG-silane were then added 30 min later and the reaction was maintained at 70 ^{o}C for 2.5 h. Extraction of CTAB were conducted in 25 mL of ethanolic ammonium nitrate (6 mg/mL) at 50 ^{o}C for 1.5 h. The obtained CuS@mSiO_2-PEG nanoparticles were separated by centrifuge at 18000 rpm for 10 min, washed with ethanol and water several times, and redispersed in DI water and stored at 4 ^{o}C for further use.

Synthesis of other PEGylated mesoporous coated metal sulfide nanoparticles: For the synthesis of CTAB stabilized Ag_2S and HgS, Na_2S (50 mM, 0.2 mL) and $AgNO_3$ (200 mM, 0.1 mL) or $HgCl_2$ (100 mM, 0.1 mL) aqueous solution were injected into a 12 mL CTAB aqueous solution (0.25 mg/mL) at 35 ^{o}C, forming a brown homogenous solution. The solution was degassed and heated to 90 ^{o}C and maintained for 30 min under a genteel nitrogen flow.

For the synthesis of CTAB stabilized CdS, Na_2S (50 mM, 0.25 mL) and $CdCl_2$ (50 mM, 0.25 mL) aqueous solution were injected into a 12 mL CTAB aqueous solution (2 mg/mL) at 35 ^{o}C, forming a yellow homogenous solution. The solution was degassed and heated to 90 ^{o}C and maintained for 30 min under a genteel nitrogen flow.

After that the solution was diluted to a total volume of 50 mL and extra CTAB was added to make the total CTAB concentration at 2 mg/mL. The subsequent coating procedure was the same as for CuS nanoparticles.

Synthesis of Au NRs and Au NR@ mSiO_2-PEG: gold nanorods (Au NRs) were synthesized according to a previous reported seeded growth method.[1] The seed solution was prepared mixing 0.6 mL of fresh prepared 0.01 M $NaBH_4$ with 5 mL of 0.5 mM $HAuCl_4$ and 5 mL of 0.2 M CTAB solution. The seed solution was aged at room temperature for 30 min after 2 min stir. To prepare the growth solution, 4.5 g of CTAB and 0.617 g of sodium oleate were dissolved in 125 mL water at 50 ^{o}C. Then 12 mL of 4 mM $AgNO_3$ was added after the solution was cooled down to 30 ^{o}C. The solution was then kept undisturbed for 15 min, and after that 125 mL of 1 mM $HAuCl_4$ was added. 1 mL of concentrated HCl was added after 90 min of genteel stirring. After 15 min, 625 μL of 0.064 M ascorbic acid was added and stirred for 30 s. At last, 150 μL of seed solution was added and further stirred for 30 s. The solution was kept at 30 ^{o}C for 12 h and then centrifuged at 7,000 rpm for 30 min and washed with water once. The obtained Au NRs were finally dispersed in 10 mL of water and 4 mL Au NRs solution was taken for mesoporous silica coating. The coating process was the same as other materials mentioned above.

Measurement of Photothermal Performance: An aqueous dispersion of CuS@mSiO_2-PEG nanoparticles (300 uL) with different concentrations was added into a 96-well plate. 980 nm stabilized infrared fiber laser with a beam diameter around 6 mm (LEO Photonics) were used to irradiate the nanoparticle dispersions. The temperature of the solution was measured every minute with a TM902C thermodetector.

In Vitro photothermal ablation of cancer cells: HeLa cells (350,000 cells) were seeded onto a 35 mm confocal dish at 37 ^{o}C with 5% CO_2 in complete medium one day before the treatment. Then, the cancer cells were washed with PBS and incubated with CuS@mSiO_2-PEG nanoparticles with a concentration of 100 ug/mL for 3 hours. A 980 nm laser with a power density of 2.4 W/cm^2 were used to irradiate the cells. After 4 min, the nanoparticles were removed and cells were further incubated in complete medium for 12 h. The cells were than washed with PBS and stained with calcein AM and PI according to the manufacturer's suggested protocol for CLSM imaging.

Drug loading and release: 2 mL as-prepared nanoparticles (1mg/mL) and 0.5 mg DOX in 1mL DI water were mixed together and stirred genteelly for 24 h. The loaded nanoparticles were then collected by centrifugation at 18000 rpm for 10 min and washed with water twice. The loading amount was determined by UV-vis absorbance at 480 nm. The DOX loaded nanoparticles were then diluted in different buffers to an equivalent DOX concentration of 5 ug/mL. To monitor the real-time release behavior, the fluorescent intensity of the diluted sample at 555 nm was directly recorded on fluorescence spectrometer with an excitation wavelength at 480 nm. To evaluate the effects of NIR-light on the release behavior, the suspension was placed in a cuvette and irradiated with 980 nm laser for 10 min with a power density of 2.4 W/cm^2. The samples were then centrifuged at 18000 for 10 min and the supernatant were collected for fluorescent measurement (excited at 480 nm). Note that, the emission intensity is in linear correlation with DOX concentration in our detection range (Fig. S16).

Intracellular DOX release: HeLa cells were seeded in a 35 mm confocal dish and cultured for 24h. Then the culture medium was removed and DOX loaded nanocomposites in fresh culture medium with a DOX concentration of 5 ug/mL was added. After incubated for 1 h, the cells were washed with PBS three times and stained with Hoechst 33342 (2 ug/mL) for 15 min at 37 ^{o}C. After three times wash with PBS, CLSM observation was carried out.

Cell Viability studies: HeLa cells were seeded in 96-well plates (1×10^5 cells/well) and cultured for 24 h before experiment. Then, the cancer cells were incubated with nanoparticles (with and without drug) with different concentrations for 3 hours. 980 nm laser at a power density of 2.4 W/cm^2 were used to irradiate the cells for 3 min each well. After wash with PBS, fresh complete medium were added and the cells were further cultured for 24 h. After this, a standard MTT assay was applied to determine the cell viabilities. Absorbance intensity at 490 nm was determined with Varioskan flash multimode reader (Thermo Scientific). Four replicates were done for each group.

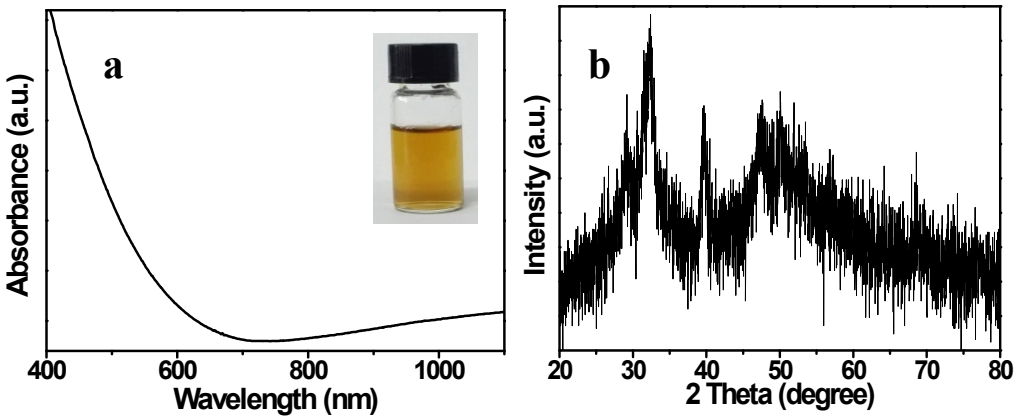

Fig. S1 Absorption spectra (a) and XRD pattern (b) of CTAB stabilized $Cu_{2-x}S$ nanoparticles, the inset shows a photograph of $Cu_{2-x}S$ nanoparticles in water. The major peaks of XRD pattern can fits to $Cu_{1.96}S$ (029-0578), but not all the peaks. The obtained nanoparticles should be a mixed phase of copper sulfide, thus denoted as $Cu_{2-x}S$ here. According to our previous work, the low extinction of the nanoparticles in the NIR range also indicates the nanoparticles here are closer to Cu_2S rather than CuS.[2]

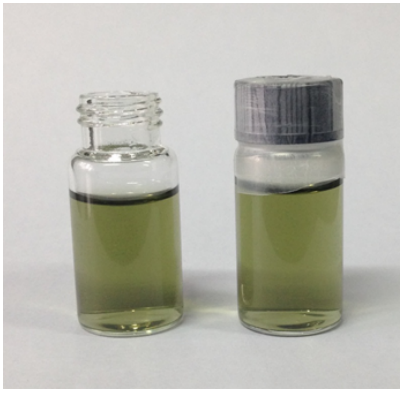

Fig. S2 Photographs of $Cu_{2-x}S$ nanoparticles (left: exposed to air; right: sealed) after 4 days storage at room temperature, they turned into CuS itself without heating. We speculate that CuS is thermodynamically more stable stoichiometry under our reaction condition than $Cu_{2-x}S$, therefore CuS was formed as a result of copper loss from $Cu_{2-x}S$ and rearrangements of the sulfur atoms,[2] and this process can be accelerated by heating them to 90 ^{o}C.

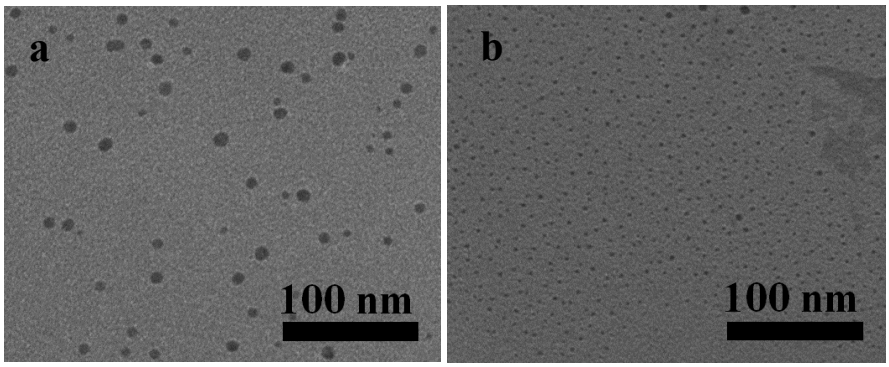

Fig. S3 (a) TEM images of $Cu_{2-X}S$ nanoparticles before heating to 90 °C. (b) CTAB stabilized CuS nanoparticles prepared with an initial CTAB concentration of 2 mg/mL.

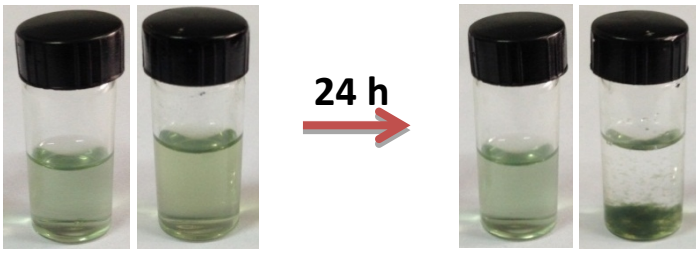

Fig. S4 Photographs of mesoporous silica coated CuS nanoparticles with (left) and without (right) PEG coating suspended in DI water, and after they were stored for 24 h.

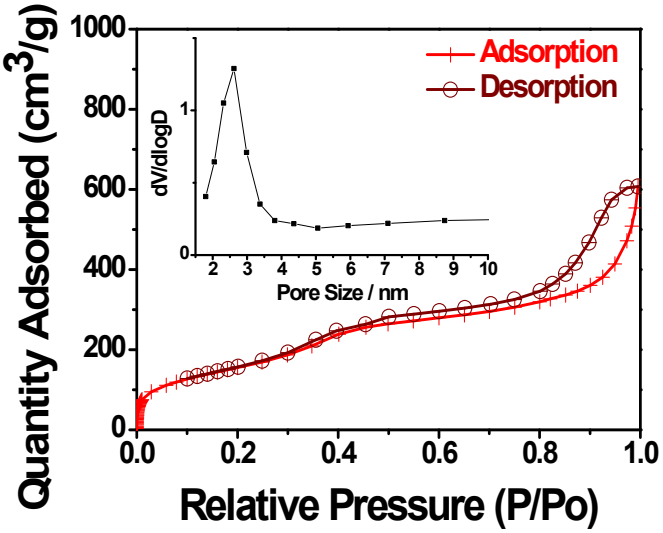

Fig. S5 Nitrogen adsorption-desorption isotherms of CuS@mSiO_2-PEG nanoparticles (inset: pore size distribution).

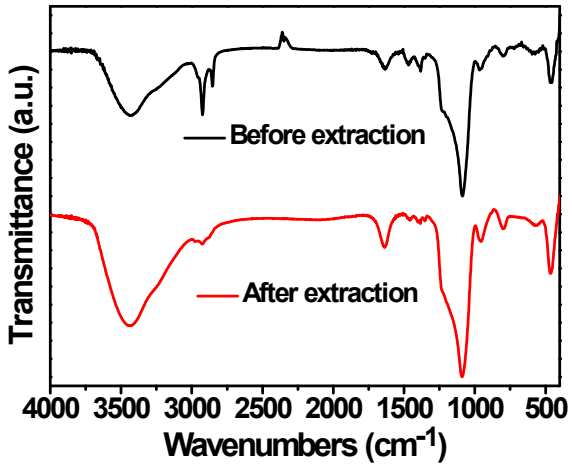

Fig. S6 FITR spectrum of CuS@mSiO_2-PEG nanoparticles before and after CTAB exctration.

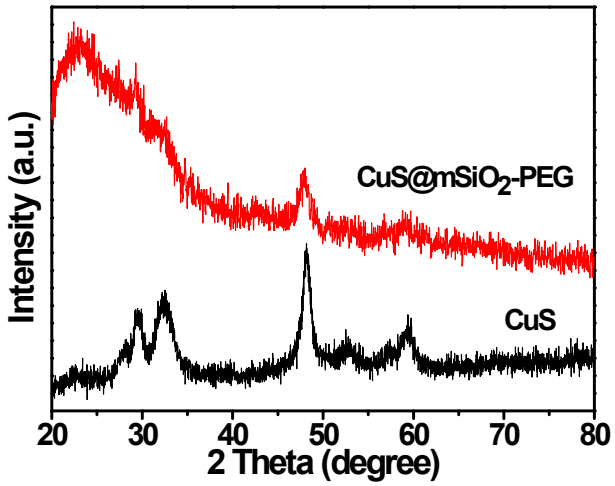

Fig. S7 XRD patterns of as-prepared CuS and CuS@mSiO_2-PEG nanoparticles, which can be indexed as covellite phase CuS (JCPDS: 079-2321).

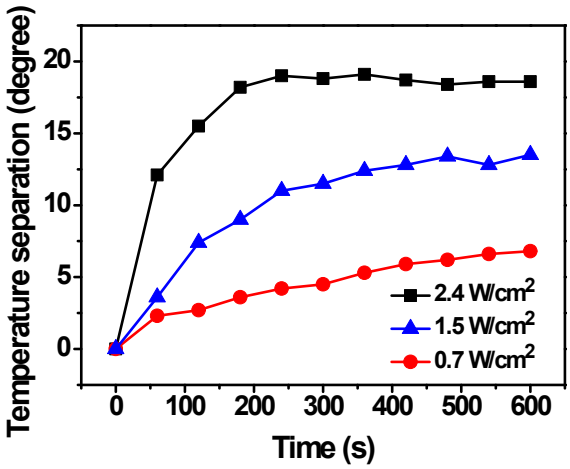

Fig. S8 The temperature separation between CuS@mSiO$_2$-PEG (100 ug/mL) and water irradiated with 980 nm later with different power densities.

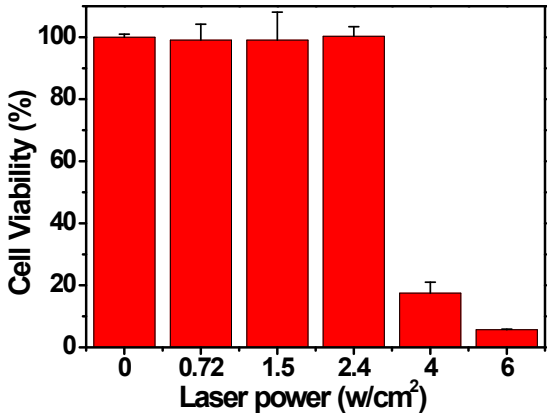

Fig. S9 Cell viabilities of HeLa cells irradiated with a 980 nm laser for 3 min at different power densities. The death of cells under high power laser is similar with the previous report.[3]

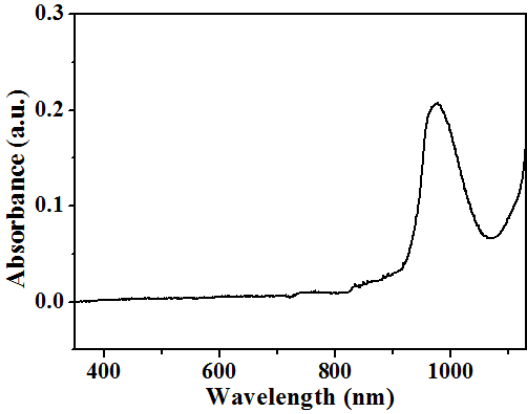

Fig. S10 Absorption spectra of pure water, showing a relatively high absorption peak around 980 nm.

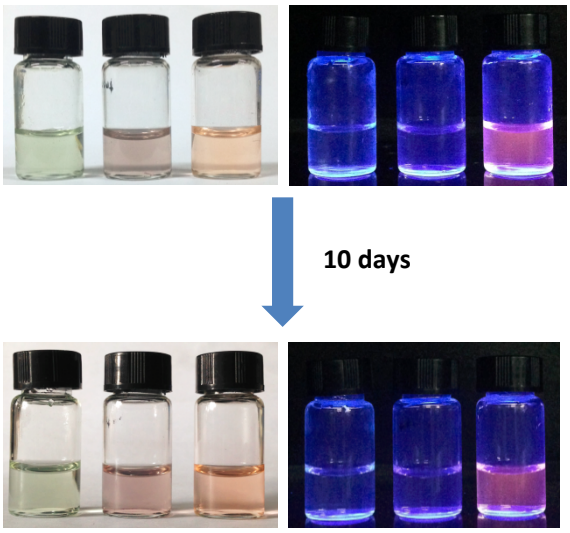

Fig. S11 Photographs of CuS@mSiO$_2$-PEG, DOX loaded CuS@mSiO$_2$-PEG and free DOX (from left to right) at an equivalent nanoparticle and DOX concentration under room light (left) and UV light (right). The negligible color change after 10 days indicates the good stability of the nanoparticles. Non emission of DOX loaded CuS@mSiO$_2$-PEG under UV light after 10 days indicates no drugs were leaking from the nanoparticles.

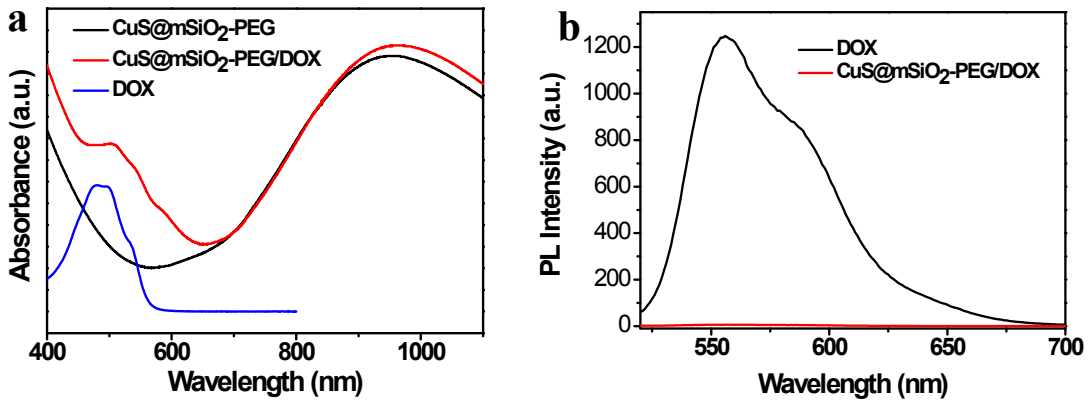

Fig. S12 (a) Absorption spectra of CuS@mSiO$_2$-PEG nanoparticles before and after DOX loading. (b) Fluorescent spectra of DOX loaded CuS@mSiO$_2$-PEG and free DOX at an equivalent DOX concentration.

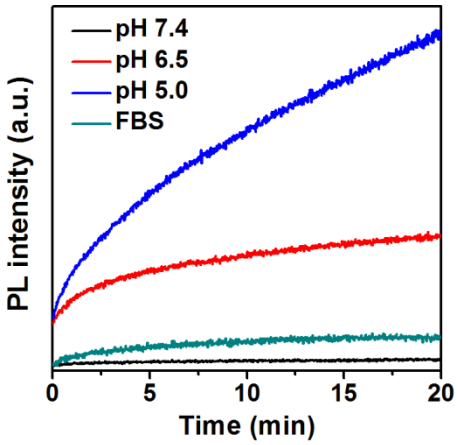

Fig. S13 Real time monitoring of the drug release from the nanocarrier under different pHs and in FBS.

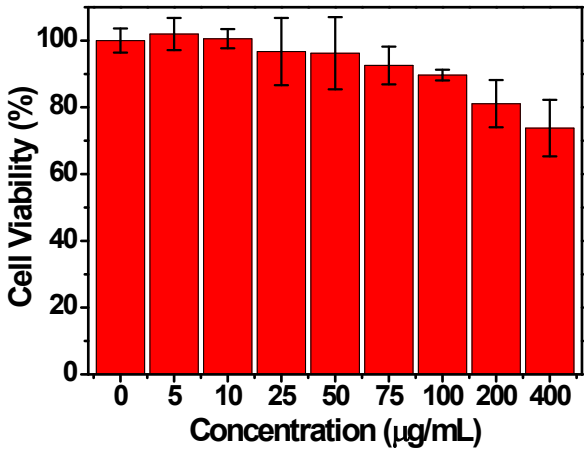

Fig. S14 Cell viabilities of HeLa cells incubated with CuS@mSiO_2-PEG nanoparticles at different concentrations for 24 h. Higher than 90% cell viability remained when the concentration is below 100 ug/mL.

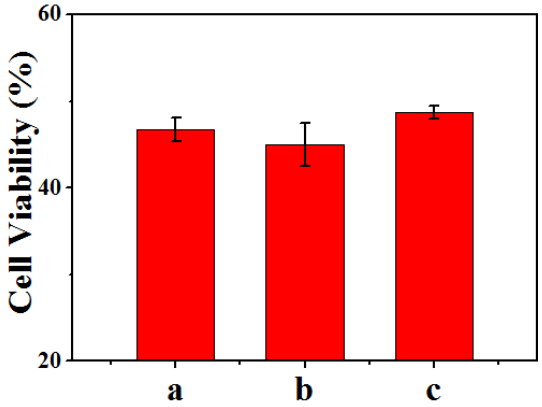

Fig. S15 Cell viabilities of HeLa cells after simultaneously applied photothermal-chemo treatment (b) and sequentially applied photothermal-chemo (a), chemo-photothermal (c) treatment, the nanocomposites applied was 50 μg/mL, nanocomposites without DOX was used for photothermal treatment. The data suggests that the simultaneously applied photothermal-chemo treatment provides a higher therapeutic effect.

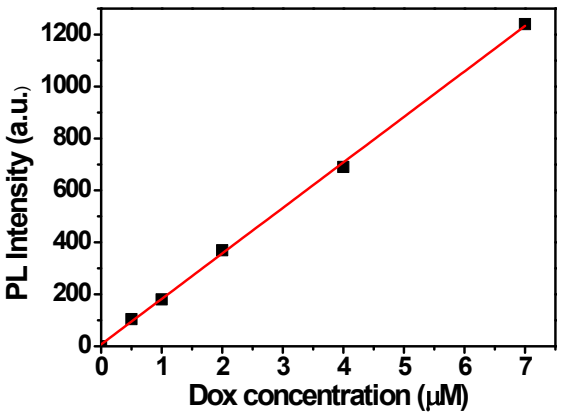

Fig. S16 Calibration curve between the emission intensity and the concentration of DOX.

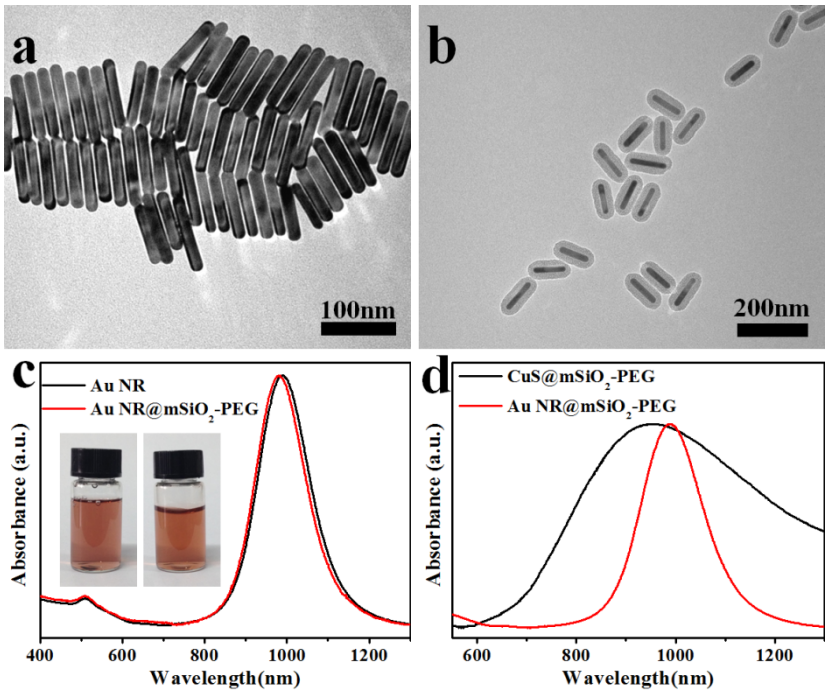

Figure

Fig. S17 TEM images (a, b) and UV-vis spectra (c) of Au NR and Au NR@mSiO$_2$-PEG nanoparticles. Inset in (c) shows the photographs of Au NR and Au NR@mSiO$_2$-PEG nanoparticles dispersed in DI water and no precipitate was observed after one week. (d) The absorption spectra of CuS@mSiO$_2$-PEG and Au NR@mSiO$_2$-PEG in the NIR range.

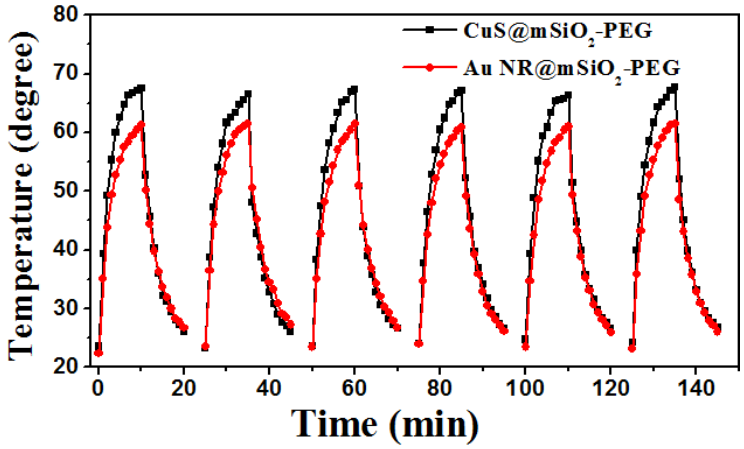

Fig. S18 Temperature change of CuS@mSiO$_2$-PEG and Au NR@mSiO$_2$-PEG nanocomposites over six LASER (980 nm, 2.4 W/cm^2) ON/OFF cycles (the next cycle started when the solution temperature cooled down to the room temperature). The absorbance of both nanocomposites was adjusted to 0.5 at 980 nm before irradiation.

By exploring the literature and comparing the properties of CuS@mSiO$_2$-PEG and Au NR@mSiO$_2$-PEG (Fig. S17 and S18), we found that although the gold nanorods as a noble metal are supposed to be more stable against oxidizing agent and strong acid,[4, 5] CuS-based nanocomposites shows more advantages. First, CuS is much less expensive than gold, the cost for the synthesis of CuS is only 1% for that of gold.[6] Second, synthesis of Au NRs is much more complicated and time-consuming than CuS.[1] Third, CuS and CuS@mSiO$_2$-PEG have much broader absorption peak in the near infrared range which makes them easily compatible with commonly used lasers for *in vivo* photothermal therapy.[7, 8] Although the surface plasmon absorption peak of Au NR can be tuned, it is still not easy to accurately control their absorption position to match the wavelength of the laser due to their sharp absorption peak and batch to batch difference. Furthermore, as the surface plasmon will be affected by the solvent or surrounding environment, the absorption of Au NR may shift *in vivo* which can lead to the mismatch with the laser and lower the photothermal efficiency.[6, 9] With a very broad absorption peak, CuS nanocomposites will be much less affect by this issue. Fourth, the CuS nanoparticles have a small size. The CuS nanoparticles synthesized in this work is within 15 nm and they are still within 50 nm after mesoporous silica coating, which is suitable for bio-medical applications. In comparison, Au NR requires larger size (typically 50 nm in length)[10] to shift their absorption into near infrared range for photothermal therapy. Here, to achieve a similar absorption peak with CuS, the size of gold nanorods need further increased to ~90 nm in length. After silica coating, the total length exceed 110 nm which is not optimal for biomedical applications. Fifth, CuS@mSiO$_2$-PEG was found to have higher photothermal conversion efficiency than Au NR@mSiO$_2$-PEG (Fig. S18). CuS@mSiO$_2$-PEG exhibited higher elevated temperature than Au NR@mSiO$_2$-PEG after 10 min irradiation, indicating higher photothermal conversion efficiency. Interestingly, both of the nanocomposites show excellent photothermal stability within 6 laser ON and OFF cycles, although several reports showed Au NRs will melt into nanospheres and temperature elevation will decrease significantly within 5-6 cycles.[11, 12] This phenomenon indicates that mesoporous silica coating can stabilize the core and provide high photothermal stability, which further demonstrates photothermal agent coated with a PEGylated mSiO$_2$ layer is a highly efficient and reliable platform for the combination of photothermal and chemotherapy.

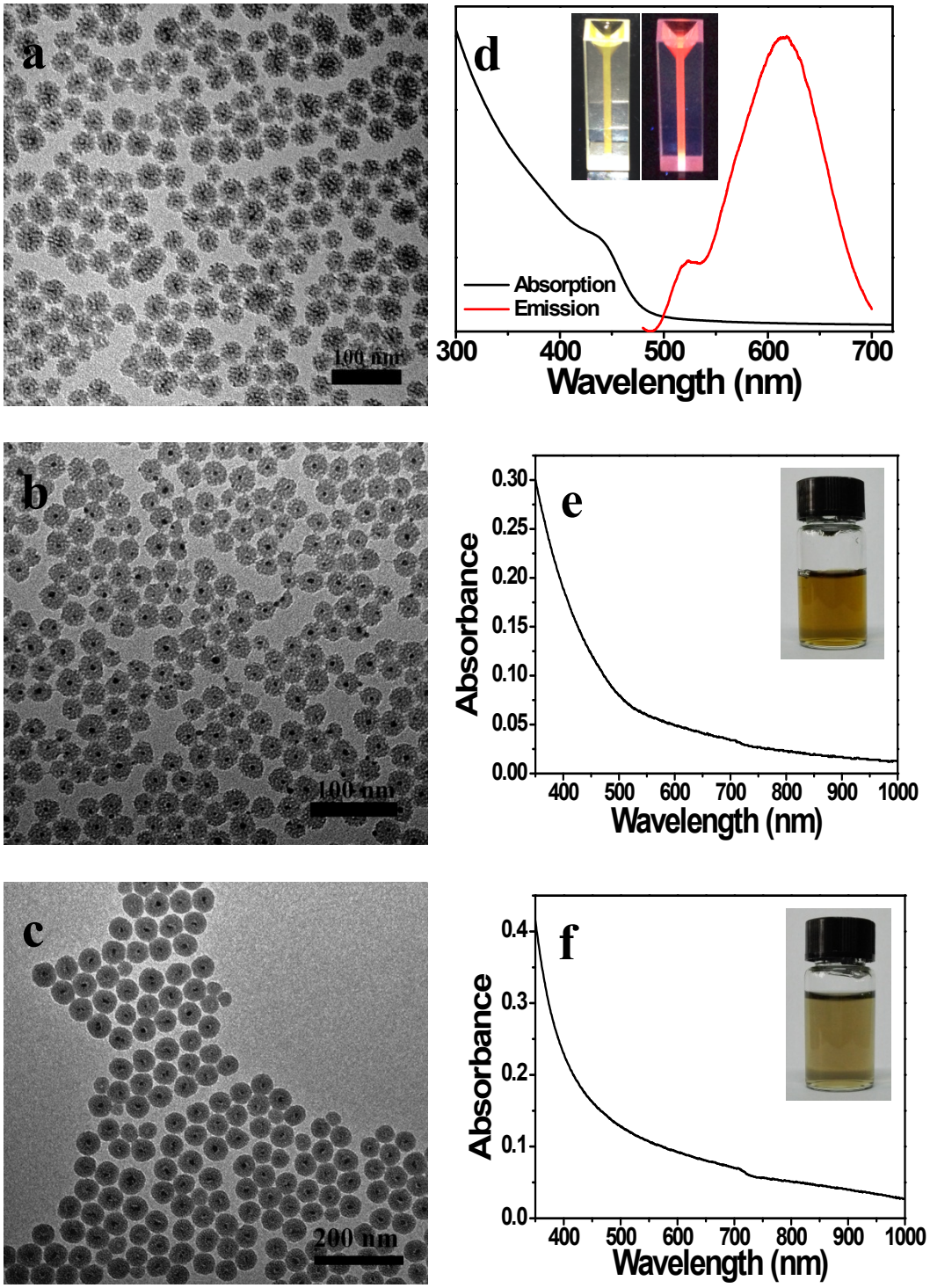

Fig. 19 TEM images (a, b, c) and absorption spectra (d, e, f) of PEGylated mesoporous silica coated CdS, Ag_2S and HgS nanoparticles (Inset shows the photographs of the samples). As CdS nanoparticles are emissive here, fluorescent spectrum and photograph under UV light were also provided in (d). The emission at around 600 nm can be assigned to deep trap emission.[13]

Reference:

1. X. C. Ye, C. Zheng, J. Chen, Y. Z. Gao and C. B. Murray, *Nano Lett.* , 2013, **13**, 765-771.
2. Y. X. Zhao, H. C. Pan, Y. B. Lou, X. F. Qiu, J. J. Zhu and C. Burda, *J. Am. Chem. Soc.* , 2009, **131**, 4253-4261.
3. X. J. Xie, N. Y. Gao, R. R. Deng, Q. Sun, Q. H. Xu and X. G. Liu, *J. Am. Chem. Soc.* , 2013, **135**, 12608-12611.
4. E. C. Dreaden, A. M. Alkilany, X. H. Huang, C. J. Murphy and M. A. El-Sayed, *Chem. Soc. Rev.* , 2012, **41**, 2740-2779.
5. Y. Xie, A. Riedinger, M. Prato, A. Casu, A. Genovese, P. Guardia, S. Sottini, C. Sangregorio, K. Miszta, S. Ghosh, T. Pellegrino and L. Manna, *J. Am. Chem. Soc.* , 2013, **135**, 17630-17637.
6. Y. Li, W. Lu, Q. Huang, M. Huang, C. Li and W. Chen, *Nanomedicine (Lond)*, 2010, **5**, 1161-1171.
7. Q. W. Tian, F. R. Jiang, R. J. Zou, Q. Liu, Z. G. Chen, M. F. Zhu, S. P. Yang, J. L. Wang, J. H. Wang and J. Q. Hu, *Acs Nano*, 2011, **5**, 9761-9771.
8. M. Zhou, G. Ku, L. Pageon and C. Li, *Nanoscale*, 2014, **6**, 15228-15235.
9. S. Ramadan, L. R. Guo, Y. J. Li, B. F. Yan and W. Lu, *Small*, 2012, **8**, 3143-3150.
10. C. M. Hessel, V. P. Pattani, M. Rasch, M. G. Panthani, B. Koo, J. W. Tunnell and B. A. Korgel, *Nano Lett.* , 2011, **11**, 2560-2566.
11. Q. W. Tian, J. Q. Hu, Y. H. Zhu, R. J. Zou, Z. G. Chen, S. P. Yang, R. W. Li, Q. Q. Su, Y. Han and X. G. Liu, *J. Am. Chem. Soc.* , 2013, **135**, 8571-8577.
12. Z. B. Zha, X. L. Yue, Q. S. Ren and Z. F. Dai, *Adv. Mater.* , 2013, **25**, 777-782.
13. Z. Li, Y. J. Ji, R. G. Xie, S. Y. Grisham and X. G. Peng, *J. Am. Chem. Soc.* , 2011, **133**, 17248-17256.